2-20-2000

NICMOS Narrowband Infrared Photometry of TW Hydrae Association Stars

David Weintraub
Vanderbilt University

Didier Saumon
Vanderbilt University

Joel H. Kastner
Rochester Institute of Technology

Thierry Forveille
Observatoire de Grenoble

Recommended Citation
David A. Weintraub et al 2000 ApJ 530 867 https://doi.org/10.1086/308402

THE ASTROPHYSICAL JOURNAL, 530:867–874, 2000 February 20

NICMOS NARROWBAND INFRARED PHOTOMETRY OF TW HYDRAE ASSOCIATION STARS

DAVID A. WEINTRAUB,[1] DIDIER SAUMON,[1] JOEL H. KASTNER,[2] AND THIERRY FORVEILLE[3]
Received 1999 June 7; accepted 1999 October 6

ABSTRACT

We have obtained 1.64, 1.90, and 2.15 μm narrowband images of five T Tauri stars in the TW Hya Association (TWA) using the Near-Infrared Camera and Multiobject Spectrometer aboard the *Hubble Space Telescope*. Most of the T Tauri stars in our study show evidence of absorption by H_2O vapor in their atmospheres; in addition, the low-mass brown dwarf candidate, TWA 5B, is brighter at 1.9 μm than predicted by cool star models that include the effects of H_2O vapor but neglect dust. We conclude that the effect of atmospheric dust on the opacity is important at 1.9 μm for TWA 5B, the coolest object in our sample. The available evidence suggests that the TWA is 5–15 Myr old. Comparison of the colors of TWA 5B with theoretical magnitudes as a function of age and mass then confirms previous claims that TWA 5B is substellar with a mass in the range 0.02–0.03 $M_\odot$. The accurate single-epoch astrometry of the relative positions and separation of TWA 5A and TWA 5B reported here should permit the direct measurement of the orbital motion of TWA 5B within only a few years.

Subject headings: infrared: stars — open clusters and associations: individual (TW Hydrae) — stars: low-mass, brown dwarfs — stars: pre–main-sequence

1. INTRODUCTION

For more than a decade, the young star TW Hya has been an enigma since it lies in a region of sky apparently devoid of the raw materials to form stars, nearly 13° from the nearest dark cloud, yet it is unambiguously a classical T Tauri star (Rucinski & Krautter 1983) surrounded by a great deal of cold dust (Weintraub, Sandell, & Duncan 1989) and gas (Zuckerman et al. 1995; Kastner et al. 1997). Recently, the TW Hya mystery was solved: TW Hya, along with other T Tauri stars found in an area of $\sim$100 square degrees of the southern sky (de la Reza et al. 1989; Gregorio-Hetem et al. 1992), compose a uniquely close association of young stars known as the TW Hya Association (Kastner et al. 1997).

At a mean distance of only $\sim$55 pc, the TW Hya Association (hereafter TWA) is almost 3 times closer than the next nearest known region of recent star formation. Given the likely age ($\sim$10 Myr) of the TWA, these stars could harbor very young planetary systems with fully formed giant planets or low-mass, brown dwarf companions, and may still be surrounded by circumstellar disks. In fact, there is substantial evidence for circumstellar gas and dust around several of these stars (Weintraub, Sandell, & Duncan 1989; Zuckerman & Becklin 1993; Zuckerman et al. 1995; Kastner et al. 1997). The relative proximity and the absence of significant interstellar or intramolecular cloud extinction in the direction of the TWA make the prospects for detecting substellar companions around these nearest T Tauri stars much better than the prospects for similar searches for young low-mass companions around T Tauri stars in Taurus-Auriga, Chamaeleon, Lupus, or Ophiuchus, the next closest regions of star formation. In a recent study of the TWA, Webb et al. (1999) identified a total of at least 17 sources as members of the TWA. In addition, Lowrance et al. (1999) and Webb et al. (1999) have reported the discovery of a likely low-mass brown dwarf companion ($M \simeq 0.02\ M_\odot$) to TWA 5A (=CD $-33°7795$) in a combination of ground-based and *Hubble Space Telescope* (*HST*) observations. TWA 5B is found almost 2″ from TWA 5A; thus, despite its relative physical proximity ($\sim$100 AU) to the primary, TWA 5B is amenable to spectroscopic and astrometric studies, uncontaminated by light from TWA 5A.

In this paper, we report results from imaging the fields around five stars in the TWA, including the TWA 5 system, using the Near-Infrared Camera and Multiobject Spectrometer (NICMOS) and the *HST*. The goal of this program was to search for companions around these stars. Our choice of three narrowband filters centered at 1.64, 1.90, and 2.15 μm was designed to enable us to identify cool and low surface gravity objects, including substellar mass companions, through their likely strong signatures of H_2O absorption at 1.9 μm.

2. OBSERVATIONS

We obtained images of five star systems (Table 1) in the TWA using camera 1 (NIC1) and camera 2 (NIC2) of NICMOS between 1998 May 30 and July 12 (UT). Observations of each of the five stars were made identically. Using NIC1 and filter F164N, we imaged each target in a four-position, spiral dither pattern, with an integration time per position of 33.894 s. Three images were obtained at each position for a total integration time of 406.73 s. We carried out identical observations using NIC1 and filter F190N, with an integration time per position of 43.864 s and a total integration time of 526.37 s. Switching to NIC2 and filter F215N, we again obtained three sets of four-position dithered image suites; however, for the F215N observations we changed the starting position for the dithered image suites in order to obtain a better median-filtered image for subtraction of the thermal background. The integration time per position was 15.948 s for the NIC2 images, for a total integration time of 191.38 s.

[1] Department of Physics and Astronomy, Vanderbilt University, P.O. Box 1807, Station B, Nashville, TN 37235.
[2] Carlson Center for Imaging Science, RIT, 84 Lomb Memorial Drive, Rochester, NY 14623.
[3] Observatoire de Grenoble, B.P. 53X, 38041 Grenoble Cedex, France.

TABLE 1

MEASURED PHOTOMETRY OF TWA STARS

TWA Number	Common Name	Spectral Type[a]	F164N (mag)[b]	H (mag)[c]	F190N (mag)[b]	F215N (mag)[b]	K (mag)[c]
1	TW Hya	K7	7.50 ± 0.01	7.65 ± 0.1	7.53 ± 0.01	7.41 ± 0.01	7.37 ± 0.07
2A	CD $-29°8887$A	M0.5	7.26 ± 0.01	...	7.39 ± 0.01	7.20 ± 0.01	7.18 ± 0.07
2B	CD $-29°8887$B	M2	8.08 ± 0.01	...	8.12 ± 0.01	7.94 ± 0.01	7.99 ± 0.07
3A	Hen 600A	M3	7.52 ± 0.01	7.60 ± 0.1	7.60 ± 0.01	7.37 ± 0.01	7.28 ± 0.07
3B	Hen 600B	M3.5	7.90 ± 0.01	8.07 ± 0.1	7.98 ± 0.01	7.79 ± 0.01	7.80 ± 0.07
5A	CD $-33°7795$A	M1.5	6.93 ± 0.01	7.06 ± 0.1	7.00 ± 0.01	6.86 ± 0.01	6.83 ± 0.07
5B	CD $-33°7795$B	M8.5	11.76 ± 0.01	12.1 ± 0.1	11.83 ± 0.01	11.49 ± 0.01	11.5 ± 0.07
8A	USNO 21A	M2	7.59 ± 0.01	7.72 ± 0.1	7.66 ± 0.01	7.53 ± 0.01	7.44 ± 0.07
8B	USNO 21B	M5	...[d]	9.36 ± 0.1	...[d]	9.13 ± 0.01	9.01 ± 0.07

[a] From Webb et al. 1999.

[b] This paper.

[c] From Webb et al. 1999. Also, P. Lowrance, A. Weinberger, & G. Schneider 1999, private communication report $H = 7.2 \pm 0.1$ for TWA 5A and $H = 12.14 \pm 0.06$ and $K = 11.4 \pm 0.2$ for TWA 5B.

[d] TWA 8A and 8B are more widely spaced than the size of the NIC1 field of view; hence, at F164N and F190N we were able to obtain data only for the primary.

3. RESULTS

3.1. *Imaging*

We find no sources in any of our images other than the previously known five primaries and four secondaries, to limiting magnitudes of 18.3, 18.4, and 17.5 in the F164N, F190N, and F215N images, respectively, at distances beyond $\sim 1\farcs3$ at 1.64 and 1.90 μm and $2\farcs3$ at 2.15 μm. The images of TWA 5 (Fig. 1) reveal how easy it is to detect and image young, intermediate-mass, brown dwarf companions around stars in the TWA, even without a coronagraph. In addition, all nine imaged objects appear as point sources (with FWHM of $0\farcs14$, $0\farcs16$, and $0\farcs18$ in the F164N, F190N, and F215N images, respectively), with no evidence (after deconvolutions performed with point-spread functions [PSFs] generated using the software package Tiny Tim,[4] direct subtractions of PSFs, and examinations of azimuthally averaged radial intensity profiles [Fig. 2]) of extended emission around any of them. Thus, although some of these stars appear to be surrounded by circumstellar material (e.g., TWA 1 is surrounded by a circumstellar disk of radius $\sim 3''$ that is viewed nearly face-on; Weinberger et al. 1999; Krist et al. 1999), we conclude that these direct, narrowband images are insufficiently sensitive to image circumstellar disks around these stars.

3.2. *Photometry*

We report our photometry for these observations in Table 1. The factors used to convert from NICMOS count rates to absolute fluxes and magnitudes[5] were 5.376665×10^{-5} Jy s ADU^{-1} for the F164N filter, 4.866353×10^{-5} Jy s ADU^{-1} for the F190N filter, and 3.974405×10^{-5} Jy s ADU^{-1} for the F215N filter with zero-point flux densities of 1033, 862, and 690 Jy, respectively. Photometry was obtained by measuring the total counts within a $0\farcs5$ radius aperture and then applying a correction factor of 1.15 to compensate for the flux that falls outside of this radius.[6]

Figure 3 shows how the photometry of TWA stars through the J, H, and K broadband and the F164N, F190N, and F215N narrowband filters relates to the near-infrared spectral characteristics of late-type stars. Stars with lower effective temperatures have increasingly strong water

[4] http://scivax.stsci.edu/ krist/tinytim.html.

[5] http://www.stsci.edu/ftp/instrument_news/NICMOS/NICMOS_phot/keywords.html, version 1998 December 1.

[6] http://www.stsci.edu/ftp/instrument_news/NICMOS/nicmos_doc_phot.html.

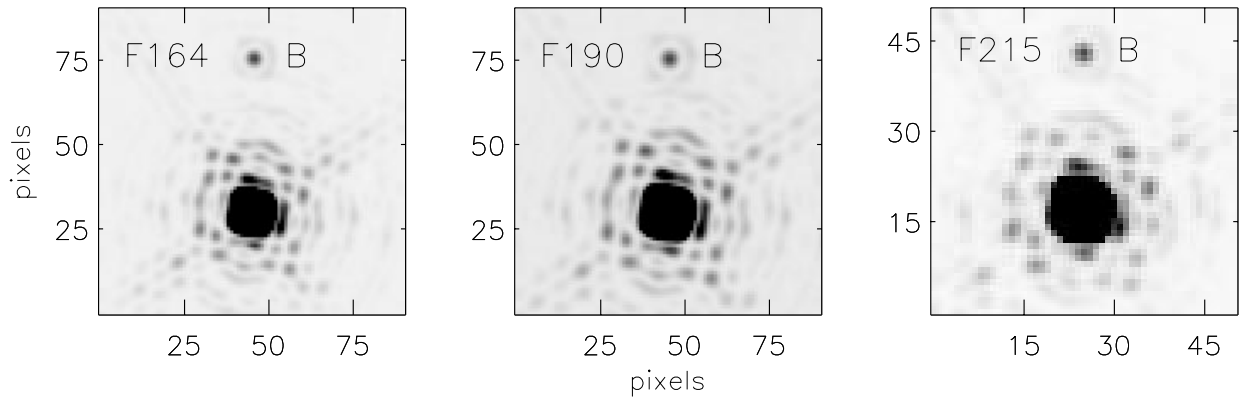

FIG. 1.—NICMOS Images of TWA 5A/B, as seen through narrowband filters at 1.64 μm (F164N) (1 pixel = $0\farcs043$), 1.90 μm (F190N) (1 pixel = $0\farcs043$), and 2.15 μm (F215N) (1 pixel = $0\farcs076$). All the small scale features seen in the images except for TWA 5B are seen identically in the model point-spread functions for NICMOS.

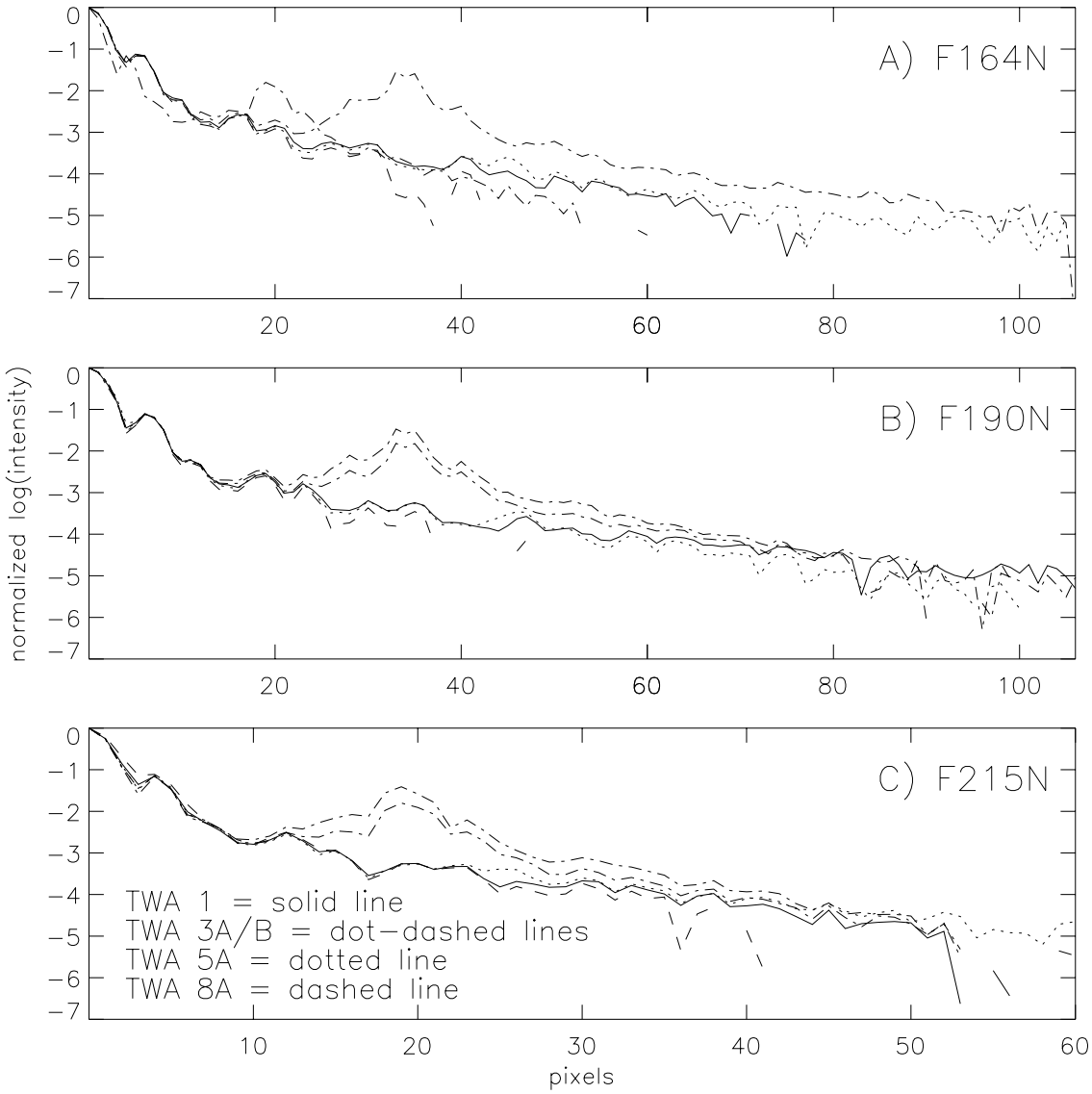

FIG. 2.—Azimuthally averaged radial intensity profiles for five of the TWA stars in our sample as seen in the (*a*) F164N (1 pixel = 0.″043), (*b*) F190N (1 pixel = 0.″043), and (*c*) F215N (1 pixel = 0.″076) filters. Each profile is normalized to the brightness of the central pixel in that profile. All profiles look identical to the PSFs generated by Tiny Tim, except for the presence of known companions.

absorption bands centered at 1.4 and 1.9 μm that are very effectively probed by this combination of broadband and narrowband filters.

We find no systematic differences between the *K* and F215N photometry (see Fig. 3, *right*), despite the slight difference in central wavelengths and large difference in bandwidth. On the other hand, the stars are systematically brighter at F164N than at *H* band, the most extreme case being TWA 5B. Finally, TWA 5B is the only star with an absolute flux that is clearly lower at 1.9 than at 2.15 μm.

The left-hand panel of Figure 3 clearly shows how water absorption in the 1.35–1.55 μm and 1.7–2.1 μm regions will strongly affect broadband *H* measurements but will have no effect on observations with the F164N filter (see also the library of near-infrared spectra published by Lançon & Rocca-Volmerange 1992). Thus, the *H* band and F164N observations reveal the presence of different amounts of water vapor absorption in the spectra of most of the stars in our sample.

3.3. *Astrometry*

For the four binary systems in our sample, we measured the intensity centroids for each binary component and transformed the cartesian positions on the array into offsets in right ascension and declination of the secondaries from the primaries (Table 2). Except for TWA 8, for which the binary separation is such that the companion only appeared in the NIC2 images, the results presented in Table 2 are those obtained using only the NIC1 images since the spatial resolution is highest when using the NIC1 array. The NIC1-based results in Table 2 are the statistical average and standard deviations based on measurements of the F164N and F190N images. The pixel to R.A. and decl. conversions were done using the plate scale measurement ephemeris generated by the NICMOS instrument team.[7] Comparison of the results for the F164N and F190N

[7] http://www.stsci.edu/ftp/instrument_news/NICMOS/nicmos_doc_platescale.html.

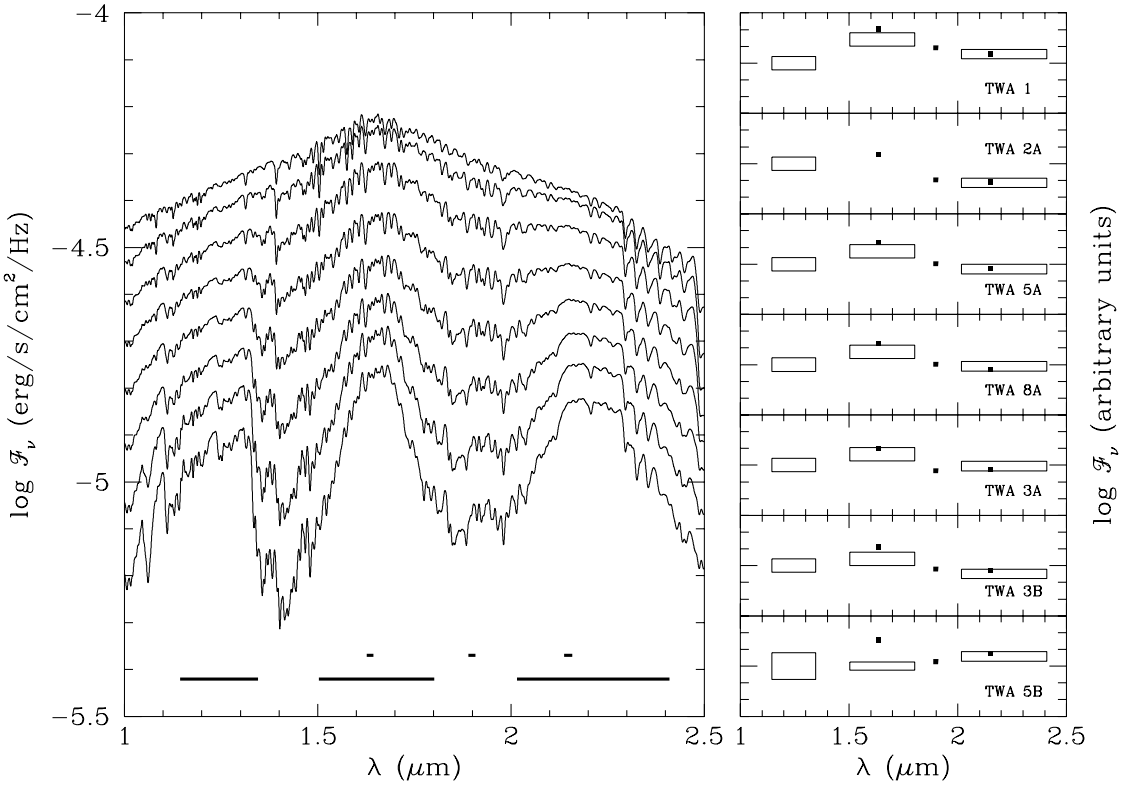

FIG. 3.—Photometry of TWA stars. *Left*: Synthetic spectra for a gravity of log $g = 4$ and $T_{\rm eff} = 4000$ K (~K7) to 2600 K (~M6), from top to bottom, respectively (Allard et al. 1996; Hauschildt et al. 1999). Bars at the bottom show the bandpasses of the Johnson-Cousin *J*, *H*, and *K* filters and of the narrowband NICMOS filters F164N, F190N, and F215N. *Right*: Broadband (Webb et al. 1999; Lowrance et al. 1999) and narrowband photometry for a representative sample of TWA stars. The photometry is expressed in arbitrary flux units, normalized to the *J* flux. Boxes show the width of the broadband filters and $\pm 1\,\sigma$ error bars. Solid squares represent narrowband photometry results. The stars are ordered by spectral type, with later types at the bottom.

images indicate that, in most cases, we can determine image separations to an accuracy of 0.02 pixels (< 1 mas).

Because our astrometric results are obtained from unocculted *HST* images and with the highest resolution camera in NICMOS, these results are much more precise than offsets previously reported for these binaries. They are, however, consistent with previous results (Table 2). In the case of TWA 5B, P. Lowrance, A. Weinberger, & G. Schnei-

TABLE 2

MEASURED BINARY SEPARATIONS[a]

Source	ΔR.A. (arcsec)	ΔDecl. (arcsec)	Separation (arcsec)	Position Angle (deg)	References
TWA 2B[b].....	+0.281 ± 0.001	+0.492 ± 0.001	0.567 ± 0.001	29.73 ± 0.03	1
	+0.3 ± 0.1	+0.5 ± 0.1	0.6 ± 0.1	31 ± 3	2
TWA 3B[c].....	−0.866 ± 0.001	−1.187 ± 0.001	1.469 ± 0.001	216.11 ± 0.03	1
	−0.8 ± 0.1	−1.2 ± 0.1	1.4 ± 0.1	214 ± 3	2
TWA 5B[d].....	−0.038 ± 0.001	+1.960 ± 0.006	1.960 ± 0.006	−1.11 ± 0.03	1
	−0.1 ± 0.1	+1.9 ± 0.1	1.9 ± 0.1	−3 ± 3	3
	−0.04 ± 0.01	+1.95 ± 0.01	1.96 ± 0.01	−1.2 ± 0.1	3
TWA 8B[e].....	−1.220 ± 0.014	−13.162 ± 0.019	13.219 ± 0.021	185.30 ± 0.06	1
	−1.3 ± 0.1	−13.0 ± 0.1	13.0 ± 0.1	186 ± 3	2

[a] From primary to secondary, based on centroid positions in NIC1 array images for TWA 2B, TWA 3B, and TWA 5B. As TWA 8B was only in the field of view in the NIC2 images, this offset is taken from those NIC2 images.

[b] NIC1 plate scale: X = 0.″0431862 pixel^{-1}, Y = 0.″0430120 pixel^{-1}, based on plate scale measurements from 1998 June 4. Observations obtained 1998 May 30.

[c] NIC1 plate scale: X = 0.″0431887 pixel^{-1}, Y = 0.″0430144 pixel^{-1}, interpolated from plate scale measurements obtained on 1998 June 4 and 1998 August 6. Observations obtained 1998 July 1.

[d] NIC1 plate scale: X = 0.″0431897 pixel^{-1}, Y = 0.″0430154 pixel^{-1}, interpolated from plate scale measurements obtained on 1998 June 4 and 1998 August 6. Observations obtained 1998 July 12.

[e] NIC2 plate scale: X = 0.″0759831 pixel^{-1}, Y = 0.″0753005 pixel^{-1}, interpolated from plate scale measurements obtained on 1998 June 4 and 1998 August 6. Observations obtained 1998 July 9.

REFERENCES.—(1) This paper; (2)Webb et al. 1999; (3) Lowrance et al. 1999, private communication. P. Lowrance, A. Weinberger, & G. Schneider 1999, private communication report corrections of the position of TWA 5B originally reported in both Lowrance et al. 1999 and Webb et al. 1999.

der (1999, private communication) recently independently determined that the offsets reported in Lowrance et al. (1999) and Webb et al. (1999) have a sign error in R.A.; the corrected values are reported in Table 2.

4. TWA 5B

4.1. *The Age of the TWA*

We have constructed an H-R diagram for the TWA (Fig. 4) using the pre–main-sequence tracks of Baraffe et al. (1998). This H-R diagram is quite similar to that presented by Webb et al. (1999), which is based on the pre–main-sequence tracks of D'Antona & Mazzitelli (1997); however, Figure 4 appears to constrain the cluster age more tightly than does previous work on the TWA, presumably because of improved physics included in the Baraffe et al. tracks (see Baraffe et al. 1997 for a discussion). Specifically, virtually all of the stars, including TWA 5B, fall between the 3 and 10 Myr isochrones. In comparison, the H-R diagrams of Webb et al. (1999) and Lowrance et al. (1999) indicate that the TWA stars have ages in the range 1–100 Myr while Kastner et al. (1997) suggested that the likely age of the TWA stars is 10–30 Myr, based on lithium studies (upper limit) and X-ray luminosities (lower limit). TWA 6 and TWA 9A, which lie together almost on the 30 Myr isochrone, and TWA 9B, which falls near the 100 Myr isochrone, are mild outliers in our and the Webb et al. (1999) HR diagrams and appear to be older than the other TWA stars (however, see Webb et al. 1999 for other possible explanations).

What other information do we have to constrain the ages of the TWA stars? Soderblom et al. (1998) used the lithium abundance to place an age range of 5–20 Myr and a most probable age of 10 ± 3 Myr on TWA 4 (HD 98800; EW(Li λ6708) = 0.36 Å); Stauffer, Hartmann, & Barrado y Navascues (1995) used the strength of the Li line to assign an upper limit of 9–11 Myr to TWA 11B (HR 4796B), while Jayawardhana et al. (1998) assigned an isochronal age of 8 ± 3 Myr to this star; and Webb et al. (1999) measured similar Li EW strengths for 14 of the 17 stars identified as members of the TWA and, on this basis, suggested that they are all less than ~10 Myr. The excellent agreement between the ages estimated from the Li EWs and those obtained from photometry and pre–main-sequence evolutionary tracks suggests that the age of the TWA is well constrained to be in the range 5–15 Myr.

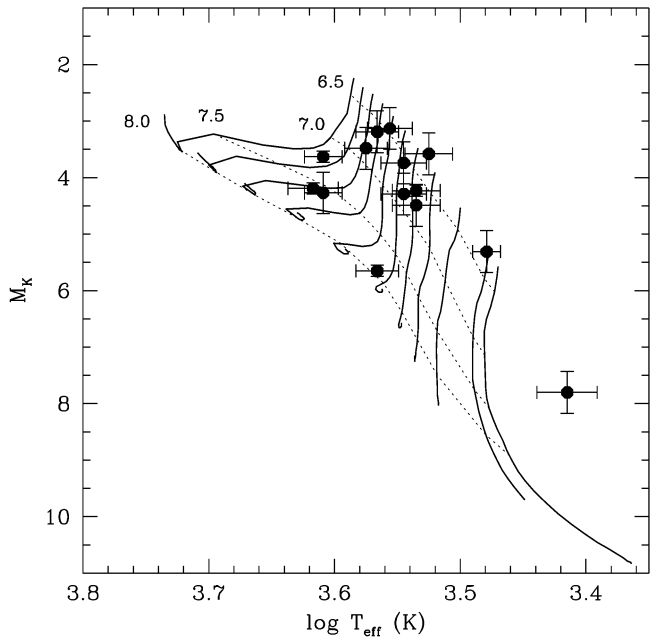

FIG. 4.—Evolutionary tracks from Baraffe et al. (1998) and the stars of the TW Hya association. Solid lines show the evolution of stars of masses from 1.0 to 0.1 $M_\odot$ in steps of 0.1 $M_\odot$ and for 0.08 $M_\odot$, from left to right, respectively. Isochrones for log t(yr) = 6.5, 7, 7.5, and 8 are shown by dotted curves. The effective temperatures of the TWA stars were obtained from the Webb et al. (1999) spectral types and the Luhman & Rieke (1998) spectral type-T_{eff} relation. The error bars on M_K reflect the uncertainties in the photometry (Webb et al. 1999) and on the distances.

4.2. *Mass and Evolutionary Status of TWA 5A and 5B*

TWA 5A is a M1.5 star (Webb et al. 1999) with T_{eff} = 3700 ± 150 K (Leggett et al. 1996). The distance to the TWA 5 system is presently unknown but can be estimated as 55 ± 9 pc from the measured parallaxes of four members of the association (Webb et al. 1999). The range of distances is consistent with the approximate angular dimension of the association. With d = 55 ± 9 pc and K = 6.8 ± 0.1, we find M_K = 3.10 ± 0.41. By comparing these values of T_{eff} and M_K with the evolution sequences of Baraffe et al. (1998), we find M = 0.75 ± 0.15 $M_\odot$ and an age of 2.5–6 Myr for TWA 5A, assuming it is a single, pre–main-sequence star (Fig. 4). On the other hand, Webb et al. (1999) report that TWA 5A is suspected to be a spectroscopic binary. If we assume that TWA 5A is binary with equal mass components, the mass of each component decreases to 0.7 ± 0.15 $M_\odot$ and the age range becomes 6–18 Myr.

Since the Baraffe et al. (1998) sequence does not extend to substellar masses, we analyze the photometric measurements of TWA 5B with evolutionary models computed by Saumon & Burrows (unpublished). These models use the same interior physics as Saumon et al. (1996) and Burrows et al. (1997) with the distinction that the surface boundary condition is provided by the "NextGen" sequence of atmosphere models computed by Allard and Hauschildt for cool stars (Allard et al. 1996; Hauschildt, Allard, & Baron 1999). The atmospheric structures provide a surface boundary condition for the interior models by giving a relation between the interior entropy (where the convective zone becomes essentially adiabatic at depth) and the surface parameters $S(T_{eff}, g)$. This relation plays a central role in controlling the evolution of fully convective stars. Colors are computed from the synthetic spectra and are therefore fully consistent with the evolution calculation. This evolution sequence was calculated for objects with solar compositions and masses between 0.01 and 0.3 $M_\odot$, and is very similar to that of Baraffe et al. (1998) since it uses the same input physics (equation of state, atmosphere models, nuclear reaction screening factors, etc.). A limitation of the "NextGen" atmospheres is that they do not include dust opacity, which becomes significant for $T_{eff} \lesssim$ <2600 K.

Figure 5 shows the evolution of the absolute magnitudes at I, J, H, and K bands, from 1 to 100 Myr, based on the models of Saumon & Burrows (unpublished). Each curve shows the evolution for a fixed mass. The two dashed lines highlight the 0.02 and 0.03 $M_\odot$ models. The boxes show the photometric measurements for TWA 5B (Webb et al. 1999; Lowrance et al. 1999), with the height of the box representing the ±1 σ photometric error and the width showing the 5–15 Myr estimated age of the association. The absolute magnitudes of TWA 5B assume a distance of 55 pc and the

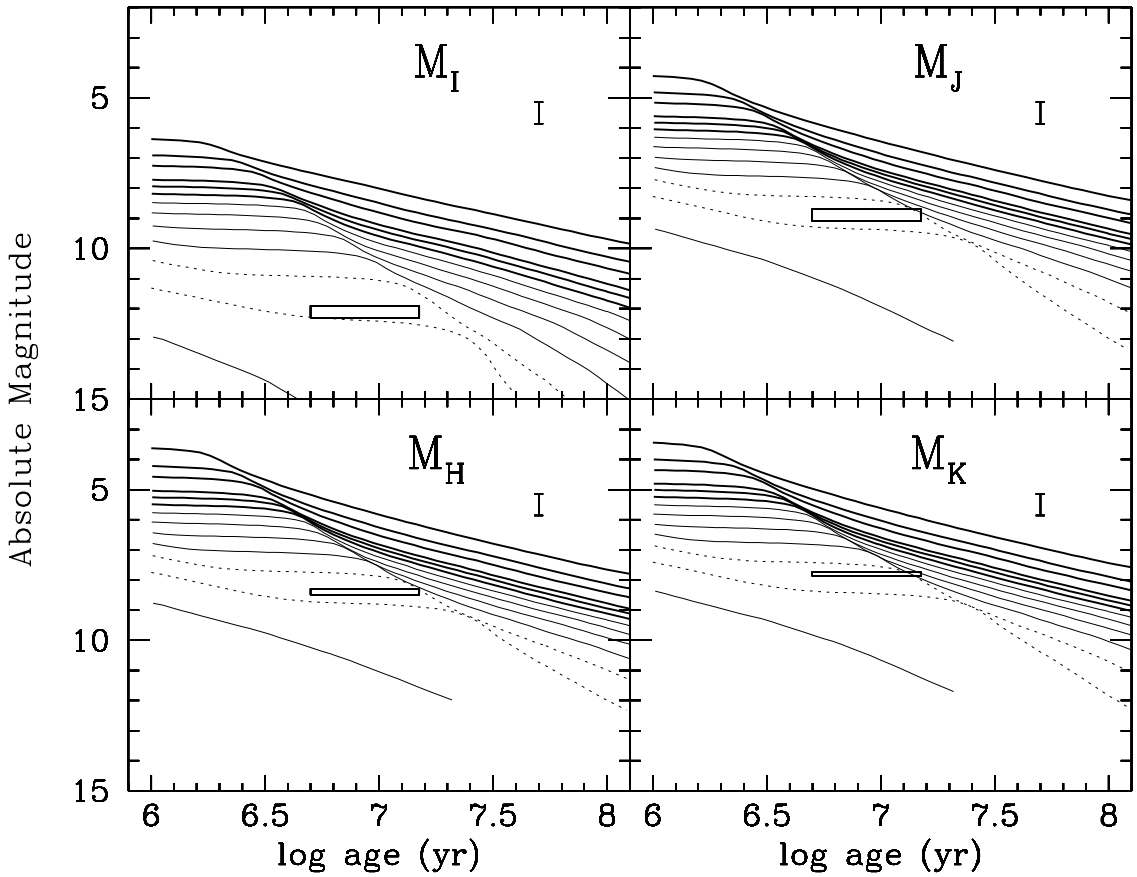

FIG. 5.—Evolution of M_I, M_J, M_H, and M_K magnitudes for very low-mass stars and brown dwarfs. From top to bottom, the curves correspond to masses of 0.2, 0.15, 0.125, 0.1, 0.09, 0.08, 0.07, 0.06, 0.05, 0.04, 0.03, 0.02, and 0.01 $M_\odot$, respectively. Heavier curves show objects with $M \geq 0.08\ M_\odot$ that eventually become main-sequence stars.

± 9 pc uncertainty is shown by the error bar in the upper right corner. All four bandpasses indicate that the mass of TWA 5B is between 0.02 and 0.03 $M_\odot$ with an upper limit of $\sim 0.06\ M_\odot$ if the TWA 5 system lies on the far side of the association and near the upper limit of our age estimate. Given this mass range and the estimated age of TWA 5B, the models indicate that its surface gravity is $3.8 \lesssim < \log g(\mathrm{cm\ s^{-2}}) \lesssim < 4.0$.

Stellar and substellar objects with $M \geq 0.012\ M_\odot$ undergo a phase of nearly constant luminosity that corresponds to the fusion of their primordial deuterium content (D'Antona & Mazzitelli 1985; Saumon et al. 1996). This phase lasts for 2–20 Myr and contraction—with a consequent steady decrease in luminosity—resumes once the deuterium is exhausted. Figure 5 shows that TWA 5B is almost certainly in the deuterium burning phase of its evolution.

4.3. *Colors of TWA 5B*

The *IJK* colors of TWA 5B are consistent with its dM8.5–dM9 spectral classification based on 0.65–0.75 μm spectra (Webb et al. 1999; Leggett, Allard & Hauschildt 1998), and thus a temperature of $T_{\rm eff} = 2600 \pm 150$ K (Luhman, Liebert, & Rieke 1997; Leggett et al. 1996). In a $J-H$ versus $H-K$ diagram, TWA 5B falls well outside of the observed sequence of very low-mass stars and brown dwarf candidates in the field (Leggett, Allard, & Hauschildt 1998), while all other members of the association fall along the observed sequence of field stars. This indicates that the H magnitude for TWA 5B may be erroneous (by $/ \geq 1\ \sigma$) or that its relatively low surface gravity results in a redder $H-K$ color.

The narrowband infrared colors are shown in Figure 6 along with the synthetic colors from the "NextGen" spectra. Each curve shows the colors for $T_{\rm eff} = 2600$, 2800, 3000, and 3200 K (from left to right) for a fixed gravity. The colors of TWA 5B are shown by the triangle with error bars. For the estimated $T_{\rm eff} = 2600 \pm 150$ K and $\log g = 3.9 \pm 0.1$, there is a reasonable agreement for the F164N–F215N color but the models are ~ 0.4 magnitude too blue in F164N–F190N. Consequently, TWA 5B is brighter at 1.9 μm than predicted by the models.

The F190N bandpass falls in the middle of a strong H_2O absorption band (Fig. 3) whose strength probably is overestimated by the "NextGen" models. Allard et al. (1997) compare a sequence of near-infrared spectra of late M dwarfs with their synthetic spectra. In all cases, the models overestimate the depth of the H_2O band, an effect that increases for later spectral types. While an inadequate H_2O opacity may be partly responsible for this effect, Tsuji, Ohnaka, & Aoki (1996) have shown that the condensation of dust in atmospheres of low $T_{\rm eff}$ results in a source of continuum opacity that decreases the depth of the water absorption bands. New atmosphere models including dust opacity (Tsuji, Ohnaka, & Aoki 1996; Leggett, Allard, & Hauschildt 1998) indicate that its effects on the spectrum (and on broadband colors) become discernible for

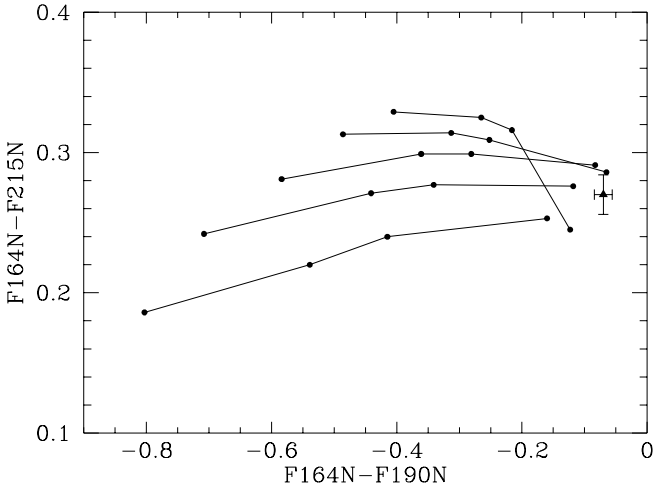

FIG. 6.—NICMOS narrowband color-color diagram. Colors calculated from the NextGen synthetic spectra (Hauschildt et al. 1999) are shown by the dots. Models with the same gravity are connected by a solid line, with log g(cgs) = 3.5 to 5.5 from top to bottom, respectively. The effective temperatures shown are 2600, 2800, 3000, and 3200 K, increasing from left to right. The observed colors of TWA5 B are shown by a triangle.

$T_{\rm eff} \lesssim < 2800$ K but remain moderate ($\sim$0.1 mag) at the effective temperature of TWA 5B ($\sim$2600 K). While current models including dust opacity may not fully account for the relatively high F190N flux of TWA 5B, the F164N–F190N color of TWA 5B is a strong indication of the presence of dust in its atmosphere.

4.4. *Astrometry of TWA 5B*

At a distance of 55 $\pm$ 9 pc, TWA 5B lies at a projected distance from TWA 5A of 108 astronomical units. TWA 5A has a spectral type of M1.5 and a likely mass for the central binary of $\sim$1.4 $M_\odot$ while TWA 5B has an estimated spectral type of M8.5 (Webb et al. 1999) and a likely mass of $\sim$25 $M_{\rm J}$. Given this information about the TWA 5 system, the orbital period P of TWA 5B should be $P \simeq 1000$ yr. Thus, the angular motion of TWA 5B, assuming a circular orbit of radius 1.″96 viewed nearly pole-on, would be 0.″013 yr^{-1} (or 0.″010 yr^{-1} if TWA 5A is a single star with a mass of 0.7 $M_\odot$ and $P = 1300$ yr).

The NICMOS observations of TWA 5 were obtained on 1998 April 25 (Lowrance et al. 1999) and 1998 July 12 (this paper), a difference of $\sim$0.21 yr. In only one-fifth of a year, the orbital motion of TWA 5B would have changed its position relative to TWA 5A by only $\sim$0.″0027, too small for the positional difference to be measured at these two epochs. Thus, the differences between the positions we measured and the corrected positions from earlier epoch observations reported by Lowrance, Weinberger, & Schneider (1999) are strictly due to the relative accuracies of the different measurements.

Although we have demonstrated that the positional change for TWA 5B is measurement error, not orbital motion, we also have shown that the position reported in this paper is a very accurate "starting" position for TWA 5B. In addition, our results show that it is possible to measure the relative separation of these two objects to an accuracy of only a few thousandths of an arcsec. Thus, the orbital motion of TWA 5B should be measurable to a fairly high degree of accuracy with ground-based observing facilities equipped with adaptive optics or with the refurbished NICMOS camera.

5. SUMMARY

To the sensitivity limits of these data, our images reveal no detectable circumstellar disks or infrared reflection nebulae, and no low-mass stellar or substellar companions around stars in the five studied TWA systems other than the previously discovered TWA 5B. As for TWA 5B itself, our results suggest that this object has a mass in the range of 0.02–0.03 $M_\odot$, in good agreement with the work of Lowrance et al. (1999). Finally, while our single-epoch observations cannot demonstrate or measure the orbital motion of TWA 5B, they are more than accurate enough to permit the measurement of this motion, in combination with future epoch *HST* or adaptive optics, ground-based observations, with a baseline of only about a year.

We thank the referee for thoughtful suggestions that improved the clarity of the manuscript, A. Burrows for computing the evolutionary sequences used in this work, and F. Allard, P. H. Hauschildt, I. Baraffe, and G. Chabrier for making their synthetic spectra and models available. This research was supported by NSF grant AST 93-18970 and NASA grants NAG 5-4988 and GO07861.01-96A and is based on observations obtained with the NASA/ESA *Hubble Space Telescope* at the Space Telescope Science Institute, which is operated by the Association of Universities for Research in Astronomy, Inc., under NASA contract NAS 5-26555.

REFERENCES

Allard, F., Hauschildt, P. H., Alexander, D. R., & Starrfield, S. 1997, ARA&A, 35, 137
Allard, F. Hauschildt, P. H., Baraffe, I., & Chabrier, G. 1996, ApJ, 465, L123
Baraffe, I., Chabrier, G., Allard, F., & Hauschildt, P. H. 1997, A&A, 327, 1054
———. 1998, A&A, 337, 403
Burrows, A., Marley, M. S., Hubbard, W. B., Lunine, J. I., Guillot, T., Saumon, D., Freedman, R. S., Sudarsky, D., & Sharp, C. 1997, ApJ, 491, 856
D'Antona, F., & Mazzitelli, I. 1985, ApJ, 296, 502
———. 1997, Mem. Soc. Astron. Italiana, 68, 4
de la Reza, R., Torres, C. A. O., Quast, G., Castillo, B. V., & Vieira, G. L. 1989, ApJ, 343, L61
Gregorio-Hetem, J., Lépine, J. R. D., Quast, G., Torres, C. A. O., & de la Reza, R. 1992, AJ, 103, 549
Hauschildt, P. H., Allard, F., & Baron, E. 1999, ApJ, 512, 377
Jayawardhana, R., Fisher, S., Hartmann, L., Telesco, C., Pina, R., & Fazio, G. 1998, ApJ, 503, L79
Kastner, J. H., Zuckerman, B., Weintraub, D. A., & Forveille, T. 1997, Science, 277, 67
Krist, J. E., Stapelfeldt, K. R., Burrows, C. J., Menard, F., & Padgett, D. L. 1999, BAAS, 31, 935
Lançon, A., & Rocca-Volmerange, B. 1991, A&AS, 96, 593
Leggett, S. K., Allard, F., Berriman, G., Dahn, C. C., & Hauschildt, P. H. 1996, ApJS, 104, 117
Leggett, S. K., Allard, F., & Hauschildt, P. H. 1998, ApJ, 509, 836
Lowrance, P. J., et al. 1999, ApJ, 512, L69
Luhman, K. L., Liebert, J., & Rieke, G. H. 1997, ApJ, 489, L165
Luhman, K. L., & Rieke, G. H. 1998, ApJ, 497, 354
Rucinski, S. M., & Krautter, J. 1983, A&A, 121, 217
Saumon, D., Hubbard, W. B., Burrows, A., Guillot, T., Lunine, J. I., & Chabrier, G. 1996, ApJ, 460, 993
Soderblom, David. R., et al. 1998, ApJ, 498, 385

Stauffer, J. R., Hartmann, L. W., & Barrado y Navascues, D. 1995, ApJ, 454, 910
Tsuji, T., Ohnaka, K., & Aoki, W. 1996, A&A, 305, L1
Webb, R. A., Zuckerman, B., Patience, J., White, R. J., Schwartz, M. J., McCarthy, C., & Platais, I. 1999, ApJ, 512, L63
Weintraub, D. A., Sandell, G., & Duncan, W. D. 1989, ApJ, 340, L69
Weinberger, A. J., Schneider, G., Becklin, E. E., Smith, B. A., & Hines, D. C. 1999, BAAS, 31, 934
Zuckerman, B., & Becklin, E. E. 1993, ApJ, 406, L25
Zuckerman, B., Forveille, T., & Kastner, J. H. 1995, Nature, 373, 494